Investigation of the electric charge structure and the dielectric permittivity at surfaces of solutions containing ionic surfactants

2006 J. Phys.: Condens. Matter 18 9823

(http://iopscience.iop.org/0953-8984/18/43/005)

INSTITUTE OF PHYSICS PUBLISHING JOURNAL OF PHYSICS: CONDENSED MATTER

J. Phys.: Condens. Matter **18** (2006) 9823–9839 doi:10.1088/0953-8984/18/43/005

Investigation of the electric charge structure and the dielectric permittivity at surfaces of solutions containing ionic surfactants

K D Schulze and H Morgner

Wilhelm-Ostwald-Institute for Physical and Theoretical Chemistry, University of Leipzig, Linnéstrasse 2, D-04103 Leipzig, Germany

E-mail: kdschulz@chemie.uni-leipzig.de

Received 27 June 2006, in final form 19 September 2006
Published 13 October 2006
Online at stacks.iop.org/JPhysCM/18/9823

Abstract

We introduce a new method for the elucidation of the electrical properties of surfaces of liquids containing surface-active salts. The approach combines two different techniques. Neutral impact collision ion scattering spectroscopy (NICISS) provides an insight into the ion distribution near the surface on a microscopic scale. On the other hand, the electrical surface potential is measured with a Kelvin probe. The results of both methods are combined to get information about the dielectric properties in the surface layer. The estimated dielectric permittivities are considerably lower than those in the bulk of the solution. The measurements have been carried out in the polar solvent formamide which contains surface-active tetrabutyl-onium salts with different anions. These salts are of interest as phase-transfer catalysts in organic synthesis.

1. Introduction

The segregation of surface-active ions in liquids causes a charged surface layer whose electrical properties can be studied [1]. The number of methods for the investigation of these properties is limited. Many experimental methods which are applied successfully in electrochemistry for studying the electrical behaviour of electrode/electrolyte interfaces are not suited for the investigation of the liquid/air interface. An example is the measurement of the interfacial capacitance. Measurements of the electrode capacitance have contributed to verify basic model ideas in electrochemistry like the Stern model of the electrochemical double layer [2, 3]. These measurements also gave evidence that the dielectric permittivity in the layer adjacent to the electrode surface (Helmholtz layer) is reduced compared to that in the bulk due to the immobilization of water molecules at the surface of the electrode. Unfortunately, this type of measurement cannot be applied to liquid surfaces.

Although the liquid/air interface differs in important details from a solid electrode/electrolyte interface, it is generally assumed that the model ideas developed in electrochemistry are principally valid for liquid interfaces, too. Still, this point requires further experimental consideration. This emphasizes the necessity to look for methods which are able to provide information about the structure of liquid interfaces. By means of neutron reflectivity Su *et al* [4] investigated the distribution of the ionic surfactant tetramethyl-ammonium-dodecylsulfate (TMADS) at the water surface. The measurements confirm the idea of an electric double layer in the surface region consisting of DS^- anions adjacent to the surface and TMA^+ counter ions distributed over a depth scale of 25 Å. The measurements showed also that large counter ions such as the TMA^+ ion are able to penetrate into the surface layer of DS^- anions and screen the repulsing forces between the surfactant ions.

Ellipsometry is used to investigate the counter ion distribution near a monolayer of surfactant ions at the water/air interface. This optical method is able to determine the positions of the counter ions which are located either in the diffuse layer or in the compact layer close to the surfactant ions. Measurements with the cationic amphiphile 1-dodecyl-4-(dimethylamino) pyridinium bromide showed that the counter ions are preferably located in the diffuse layer at low concentrations but with increasing bulk concentration a sharp transition towards a condensed state of the counter ions in the compact layer happens [5]. The same authors also studied the molecular orientation of ionic surfactants in the surface layer by using sum frequency generation spectroscopy (SFG) and molecular dynamics simulations. The results were published in a subsequent paper [6].

Siegbahn and co-workers [7] investigated the segregation of potassium octanoate in formamide with angle-resolved electron spectroscopy. The authors tried to interpret the results of the measurements on the basis of the diffuse double layer model of electrochemistry. For that purpose, they calculated the potassium ion concentration in the surface region by using the measured octanoate concentration at the surface with the help of the Poisson–Boltzmann formalism. The approach to adjust the calculated potassium surface concentration to the measured one by variation of different model parameters failed. According to the authors, this result is attributed to the simplicity of the diffuse double layer model which neglects 'closer bound cation states at the surface' in conjunction with the generation of ion pairs near the surface. Furthermore it is assumed in the model that the dielectric permittivity in the surface region agrees with that in the bulk of the solution. The authors suggest the use of a variable dielectric constant in the surface layer for forthcoming calculations.

In another paper, angle-resolved photoelectron spectroscopy (ARUPS) was used to investigate the segregation of tetrabutylammonium iodide (TBAI) in formamide [8]. The analysis of the carbon C 1s signals of the TBA^+ ions and of formamide showed that both the TBA^+ concentration and the iodide concentration are strongly enhanced at the surface. The extension of the interfacial region was found to be about 12 Å.

The same quaternary ammonium salt was studied in [9, 10] in aqueous solutions with an improved photoelectron–spectroscopic setup. A special microjet technique generates a high-speed liquid beam of some micrometres in diameter whose surface properties can be probed under vacuum conditions. Concurrently, a molecular dynamics study of the interfacial depth distribution of both the cation and the anion was carried out. The simulations showed that the depth profiles of TBA^+ and I^- overlap almost perfectly. The authors employ this result as evidence for the absence of a charged electrical double layer in the aqueous salt solution.

A technique which is able to give direct access to the ion distribution near the surface of the liquid is neutral impact collision ion scattering spectroscopy (NICISS). The combination of NICISS with the classical Kelvin probe provides a tool which enables an insight into the electrical properties of liquids on a molecular depth scale.

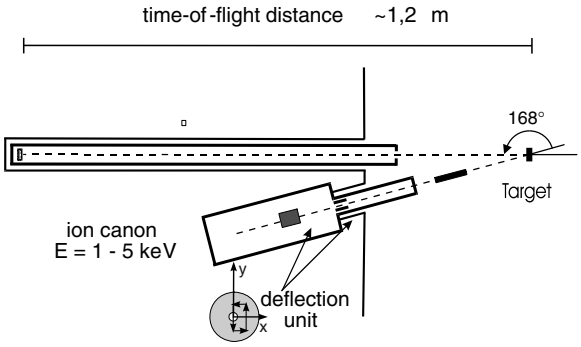

Figure 1. Experimental setup of the NICISS equipment.

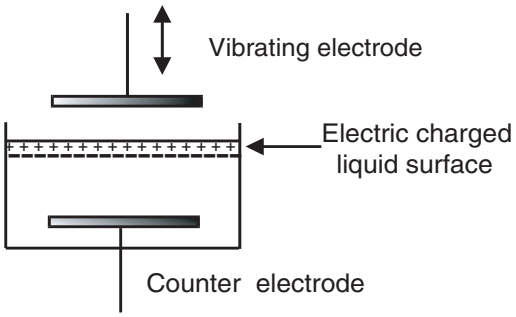

Figure 2. Scheme of the surface potential measurements by using the Kelvin probe.

2. Experimental details

The principle of NICISS is depicted in figure 1. The figure shows only the central part of the vacuum chamber, which consists of the liquid target and the ion gun for the generation of He^+ ions with the primary energy E_0 (see [11] for details). The liquid surface is created as a thin film on a rotating disc which is immersed in a reservoir containing the salt solution studied. The helium projectiles are directed to the liquid film and backscattered from the liquid. The backscattering of the projectiles is coupled with a loss of energy which depends on the mass of the target atom. Furthermore, projectiles backscattered from deeper layers lose energy on their trajectory due to interactions with matter inside the surface layer. This energy loss increases with the depth of the target atom. Therefore, the time of flight of the backscattered projectiles includes information about both the atomic mass and the depth of the atoms in the solutions.

The ion beam technique was used in the pulsed mode with a repetition time of 10 μs. The time of flight spectra were recorded with the help of a multichannel analyser with 2.46 ns channel time width.

Figure 2 shows the principle of the surface potential measurement with the Kelvin probe.

The vacuum levels of the vibrating electrode and of the liquid surface are adjusted to coincide by applying a compensating voltage U between the Fermi levels of the vibrating electrode and of the counter electrode in the liquid phase: $U = (E_{\text{Fermi,vib}} - E_{\text{Fermi,counter}})/e$. If this compensating voltage is U_1 in case of the pure solvent and U_2 in case of the solution the difference $U_2 - U_1$ measures the change of the vacuum levels in the liquid due to the presence of the surface active solute. Thus, the surface potential φ caused by the surfactant is

obtained as $\varphi = U_2 - U_1$. The given relation for φ is only valid if potential changes at the counter electrode induced by the tetrabutylphosphonium salts are negligible. Measurements with a second electrode (Ag/AgCl in KCl/formamide) as reference showed that these potential changes do not exceed some millivolts.

We use the surface potential φ to characterize alterations in the dielectric properties of the surface layer due to the segregation of ionic surfactants. This is described further below.

The surface potential measurements were carried out with a commercial Kelvin probe device from Besocke Delta Phi GmbH, Jülich, including the electrode type KPS. The vibrating electrode and the solution were placed in a Plexiglass chamber which was streamed by clean nitrogen to avoid impurities from air. The chamber was surrounded by a metal box to screen the electrode from outer electromagnetic noise. A distance of 0.5 mm between the vibrating gold electrode and the solution surface was sufficient for an optimum capacitive current for the compensation process. The formamide was supplied by Acros Organics (purity: 99.5+%). The vapour pressure of this solvent is sufficiently low for spectroscopic investigations under vacuum conditions. The surface-active salts used for the study were tetrabutylphosphonium salts (TBPX) with different anions (X = I, Br, Cl) and tetrabutylammonium chloride (TBACl). The tetrabutylammonium iodide (TBPI) was self-synthesized according to a standard procedure by using of tributylphosphine and butyliodide. The other salts were commercial products with only >97% purity. Preliminary studies showed that this purity was not sufficient for our investigations. Therefore, all salts (including TBPI) were recrystallized twice using a mixture of petroleum benzine and benzene. The recrystallization of the hygroscopic TBPCl was carried out under closed conditions to avoid any contact with water vapour from air.

3. Results

Figure 3 shows the measured time of flight spectra and the threshold position of the single elements. The spectrum of the pure formamide is characterized by steps of oxygen O, nitrogen N and carbon C belonging to the compounds of the liquid. These steps are superimposed to the spectrum for the recoil hydrogen atoms sputtered by the He projectiles. Additionally, the segregation of the salt ions to the surface gives appropriate peaks of intensity in the time of flight spectra in which ions appear in the sequence of their atomic weights. The time of flight of the backscattered He projectiles decreases with increasing mass of the scattering atoms in the liquid, as shown in figure 3.

The count rate of the spectra in figure 3 is normalized with respect to measurement period and primary beam current. In order to investigate the segregation of the surface-active salt we have to eliminate the hydrogen background in the spectra. This is done by subtracting the spectrum of pure formamide from the solvent spectra. Figure 4 shows those parts of the resulting curves which are of interest for the further analysis.

The spectra in figure 4 depicts the signal of the TBP^+ cation and the signals of the halogen anions. In the case of TBPCl both ion signals are superimposed. The separation of the signals requires information about the shape of the chlorine signal in the range of the phosphorus signal. Therefore, we have taken the same type of spectrum for the related salt tetrabutylammoniumchloride (TBACl). For this system the chlorine signal is easily to isolate. Assuming that the shape (but not the intensity) of the chlorine signal from TBACl agrees with the shape of chlorine signal of TBPCl, an extrapolation of the latter signal in the range of phosphorus and a subsequent separation of the signals of the cation and of the anion of TBPCl are possible.

The spectra of figure 4 can be used for the calculation of depth profiles of the salt ions. This calculation is explained in the next section. Finally, the results of the Kelvin probe

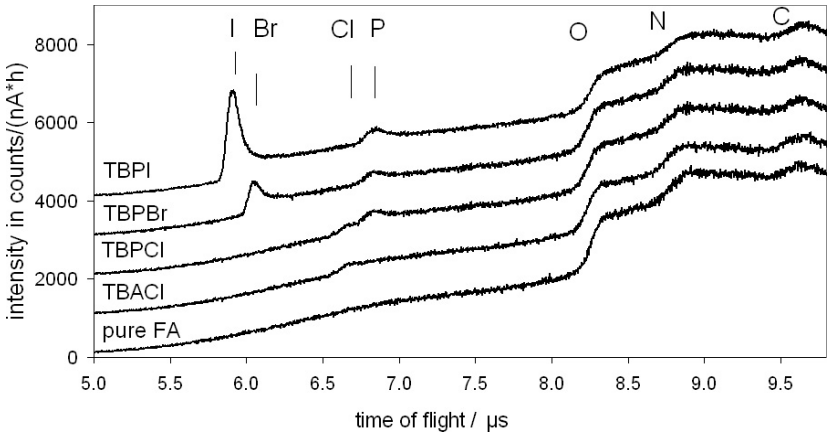

Figure 3. Time of flight spectra for formamide solutions containing 0.25 molal tetrabutylphosphonium salts TBPX (X = I, Br, Cl) and 0.25 molal tetrabutyl-ammonium chloride TBACl. The time of flight spectrum of pure formamide is given as a reference. The primary energy of the He^+ projectiles was $E_0 = 2$ keV.

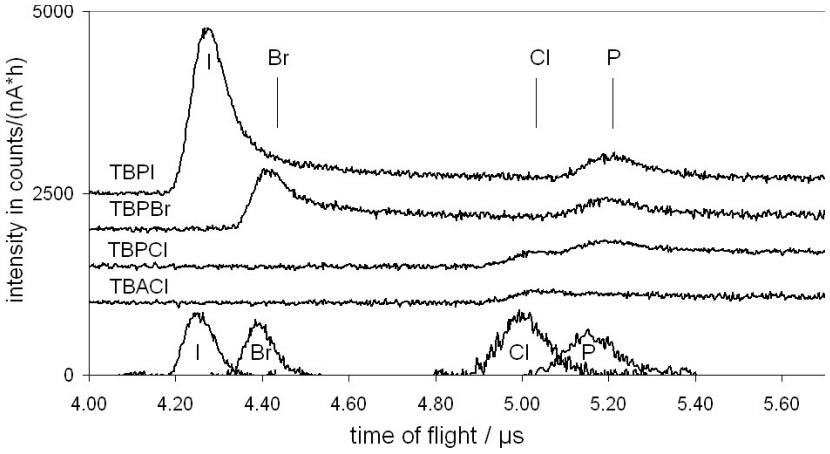

Figure 4. The time of flight spectra received by subtracting the spectrum of pure formamide from the spectra of the TBPX salt solutions. Gas phase spectra for the calibration of the depth scale of the elements are shown in the lower part of the figure. Note that the intensities of the gas phase spectra are not normalized on ion beam current and measuring time.

measurements are depicted in table 1. The surface potentials of the three salt solutions are distinct from each other. The largest surface potential was found for the TBPCl solution. The existence of an electrical surface potential fits well to the picture of a charged electrical double layer at the surface of the solutions used.

4. Analysis

The determination of the depth profiles from the time of flight spectra in figure 4 requires some operations which will be briefly explained (see [11, 13] for details).

The He projectiles lose energy during the backscattering process. The extent of energy transfer depends on the mass of the target atom. Additionally the projectiles lose energy on

Table 1. Electrical surface parameters and the surface excess of solutions containing 0.25 molal tetrabutylphosphonium salts TBPX (X = I, Br, Cl).

	TBPI	TBPBr	TBPCl
Surface potential φ (mV)	-105 ± 10	-175 ± 10	-240 ± 10
Mean dielectric permittivity ε_S in the surface layer	10(+6/−8)	15(+5/−7)	43 ± 4
Surface excess charge Q_S (μC cm^{-2})	2.3 ± 0.6	3.6 ± 0.4	6.7 ± 0.3
Surface excess according to equation (22) (10^{-10} mol cm^{-2})	1.90 ± 0.1	1.2 ± 0.1	0.50 ± 0.1

their trajectory through the bulk with a magnitude proportional to the depth of the target atom. The energy loss in the bulk is calibrated with self-assembled monolayers of alkanethiolates on gold and silver single crystals [12]. This calibration enables the determination of ion depth profiles from the energy loss of the He projectiles in the surface layer.

The position of the calculated depth profiles is only true within an error which is determined by the inelastic loss of energy of the projectiles. This quantity is unknown. Therefore, the depth-scale of the elements was gauged with gas phase experiments. The idea behind the experiments is the assumption that projectiles passing the gas phase interact with only one molecule. Therefore, the gas phase can be considered as equivalent to one monolayer of the liquid. We used different gas molecules for the zero point adjustment, namely trimethylphosphine for the element phosphorus, diiodomethane for iodine, tribromomethane for bromine and tetrachloromethane for chlorine. The spectroscopic investigation of the gas phase was carried out at the same position as those of the liquid film on the rotating disc of the target (see figure 1). Under this condition, the zero point of the depth scale of the element distribution in the surface layer results from the maximum of the gas phase spectrum. This maximum was found by fitting of a Gaussian curve to the gas phase spectrum (see [14] for details). The spectra which were used to calibrate the depth scale of the elements are depicted in the lower part of figure 4. Figures 5(a)–(c) show the calculated depth profiles whose depth scales are gauged with the help of the measured gas phase spectra.

The ion distributions in figures 5(a)–(c) show that the count rate statistics of both the phosphorus signal and the chlorine signal are not as good as the signals of bromine and iodine. This is due to the smaller scattering cross section of the former elements compared to bromine and iodine. The depth profiles of both salt ions have different centres of gravity. This difference causes an electrically charged double layer and a corresponding electric potential at the surface of the salt solutions. The calculation of the area of the ion depth profiles reveals that the amount of adsorbed cations and anions are equal within experimental error. Thus, electroneutrality in the surface layer is not violated.

In the context of the depth profile calculations a physical effect should be mentioned which influences the shape of the ion depth profiles. The beam of He projectiles which is used to probe the surface layer undergoes an energetic and spatial widening inside the layer due to low-angle scattering and other reasons [13]. This widening causes a decrease in depth resolution with increasing probing depth. The ion beam widening can be understood as a convolution of the true time of flight signal with a Gaussian curve whose full width at half maximum (FWHM) increases with increasing probing depth. Therefore, the time of flight spectra have to be deconvoluted with an appropriate Gaussian curve to compensate the described effect. The deconvolution procedure is based on a genetic algorithm which is given in [11]. The values of the FWHMs of the Gaussian curve for deconvolution can be determined from gas phase spectra as described in [14].

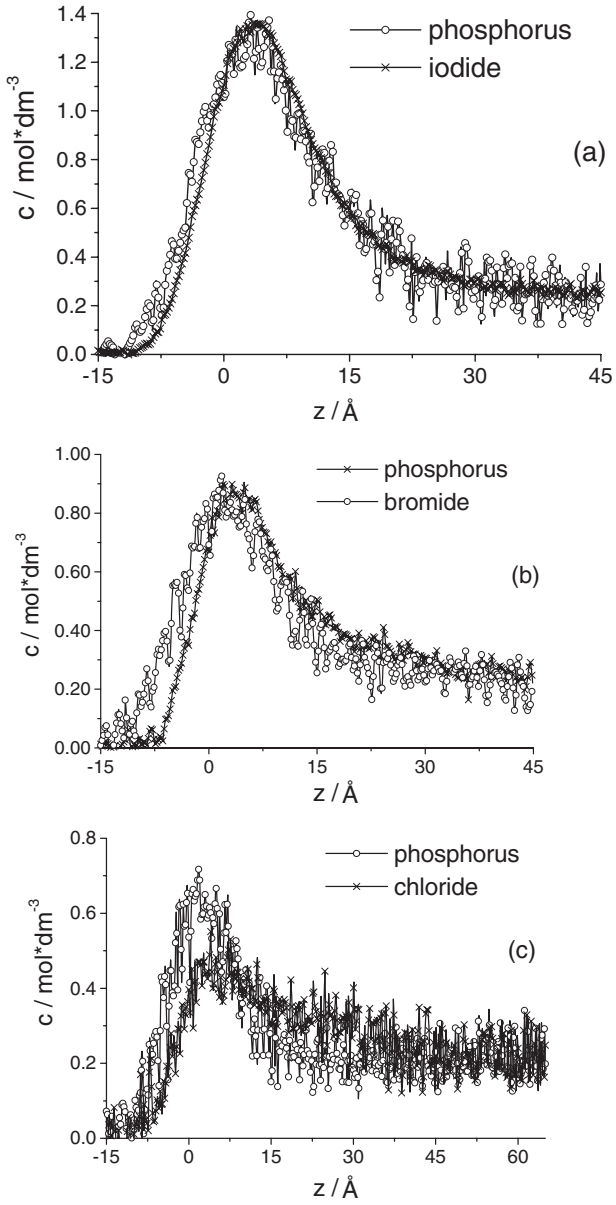

Figure 5. Ion depth profiles in the surface layer of formamide solutions containing 0.25 molal tetrabutylphosphonium salts: TBPI (curves (a)), TBPBr (curves (b)) and TBPCl (curves (c)).

Figures 6(a)–(c) show the deconvoluted ion depth profiles for the different solutions. The deconvolution of the curves influences the shape of the depth distribution of ions in the surface layer and gives narrower depth profiles compared to the ion depth profiles in figures 5(a)–(c). Note that the non-monotonic curve shape at the end of the ion depth profiles has no physical meaning but results from an increasing error of the deconvolution in this depth range.

We used the deconvoluted depth profiles and the measured electric surface potentials to estimate the dielectric permittivity in the surface layer. The calculation of the dielectric

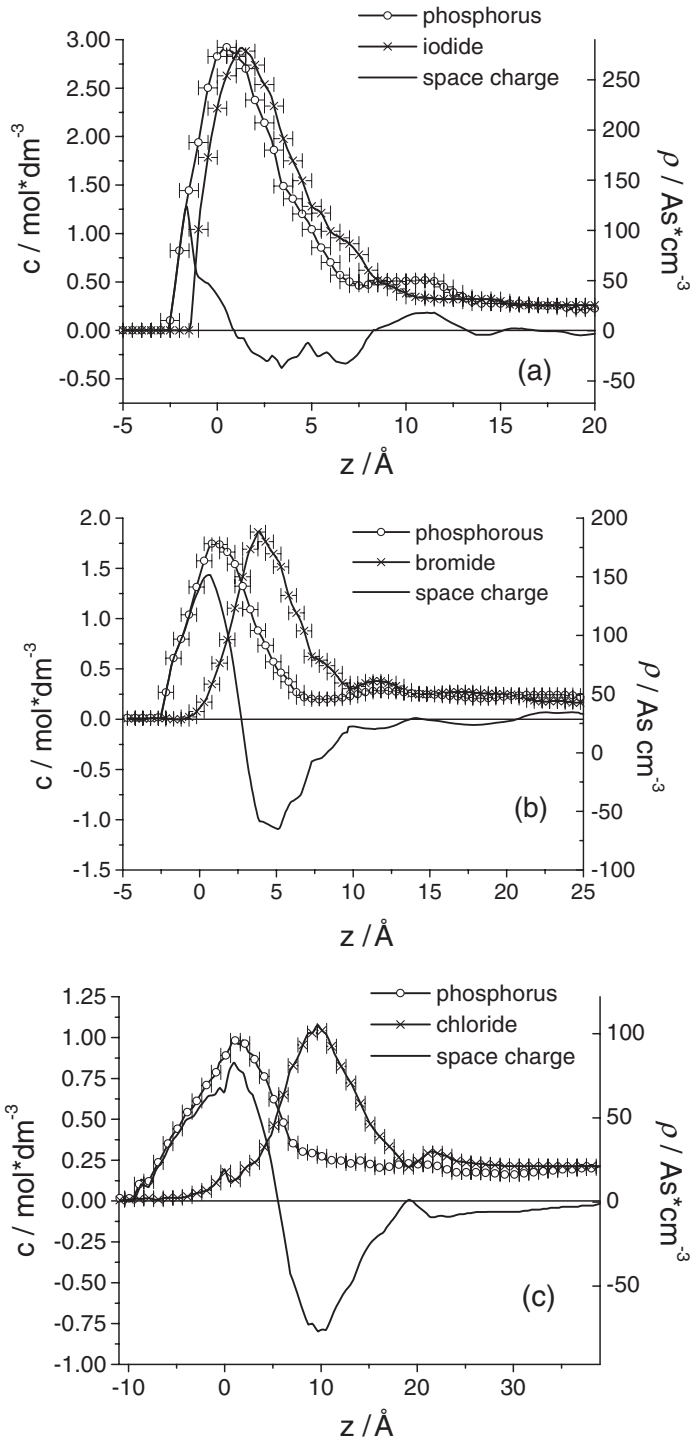

Figure 6. Deconvoluted ion depth profiles and the space charge density ρ in the surface layer of 0.25 molal solutions of tetrabutylphosphonium iodide (curve (a)), tetrabutylphosphonium bromide (curve (b)) and tetrabutylphosphonium chloride (curve (c)) in formamide.

permittivity is based on Poisson's equation of electrostatics which relates the electrical potential φ, the space charge density ρ and the dielectric permittivity of the surface layer $\varepsilon_S(z)$ according to

$$\frac{d^2\varphi(z)}{dz^2} = -\frac{\rho(z)}{\varepsilon_S(z)\varepsilon_0} \tag{1}$$

with the space charge density $\rho(z) = m_+Fc_+(z) + m_-Fc_-(z)$ containing the local concentrations of the cations $c_+(z)$ and the anions $c_-(z)$ at depth z, the charge number m of the ions, Faraday's constant F and the dielectric permittivity of free space ε_0.

The dielectric permittivity $\varepsilon_S(z)$ depends on depth due to changes of the ion concentrations and of the electric field strength inside the surface layer. This depth dependence is yet unknown and requires further model considerations (see further below).

4.1. Mean dielectric permittivity in the surface layer

As a first approximation, we regard the dielectric permittivity across the surface layer as constant. This yields the following equations for the field strength E:

$$E(z) = \frac{d\varphi(z)}{dz} = -\frac{\int^z \rho(z')\,dz}{\varepsilon_S\varepsilon_0}. \tag{2}$$

And for the electric potential $\varphi(z)$ in the surface layer, respectively,

$$\varphi(z) = \int^z E(z')\,dz' = -\frac{\int^z \left(\int^{z'} \rho(z'')\,dz''\right) dz'}{\varepsilon_S\varepsilon_0}. \tag{3}$$

Equation (3) can be used to calculate the dielectric permittivity ε_S from the experimental space charge profile $\rho(z)$ and the measured surface potential φ. A rearrangement of equation (3) yields

$$\varepsilon_S = -\left[\frac{\int^z \left(\int^{z'} \rho_1(z'')\,dz''\right) dz'}{\varphi\varepsilon_0}\right]. \tag{4}$$

The numerical integration was carried out over the whole space charge in the surface layer shown in figures 6(a)–(c). Table 1 shows the calculated ε_S for the three tetrabutylphosphonium salts.

There are strong differences between the estimated dielectric permittivities ε_S for the different salts. Possible reasons for this finding are given in the discussion.

Another electric surface parameter which can be estimated from the calculated depth profiles is the surface excess charge Q_S. In the charge layer which is directly located at the surface the number of cations exceeds the number of anions. Adjacent to this layer a charge layer with an excess of anions is located. The excess charge in both layers has to be equal by reasons of electroneutrality. Q_S can be obtained by integration of either the positive or the negative part of the space charge profiles. Table 1 shows the calculated surface excess charges for the different salts.

The presented results depend on the accuracy of the calculated depth profiles, especially on the exactness of the zero point positions of the elements. It was estimated that the error of this position is about ± 0.7 Å for the ions under study. This error corresponds to an error of the position of the cationic and the anionic depth profiles relatively to each other of about ± 1 Å according to the Gaussian error propagation. The mentioned position error influences the space charge density in the surface layer and, thus, the calculated dielectric permittivity.

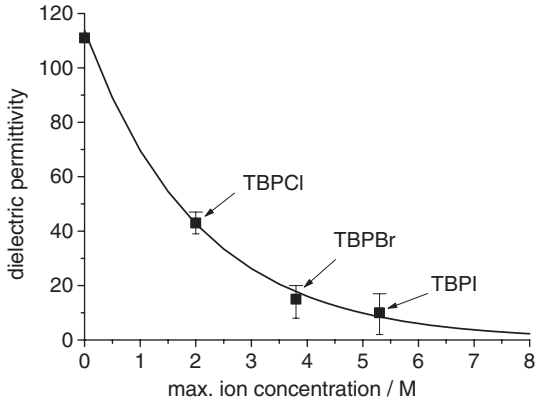

Figure 7. Mean dielectric permittivity ε_S as a function of the maximum ion concentrations in the surface layer of different salt solutions.

In an error estimation using the TBPBr curves the depth profile of phosphorus was shifted by 1 Å either into the volume of the solution (+1 Å) or towards the surface (−1 Å) whereas the position of the bromine depth profile was held constant. The numerical calculation showed that the described shift of phosphorus alters the calculated dielectric constant from 15 to 8 (+1 Å shift) and 15 to 20 (−1 Å shift), respectively. Analogous estimations using the cationic and the anionic depth profiles of TBPI and TBPCl showed that the error of the dielectric permittivity ε_S resulting from an additional 1 Å shift in the ion depth profiles is somewhat larger for TBPI and smaller for TBPCl compared to those of TBPBr (see the errors of ε_S in table 1). Another error could result from the measured surface potential. This error was estimated as ±10 mV. The given error of the measured surface potential is—with regard to the calculated dielectric permittivity—of minor importance compared to position error of the depth profiles.

In the context of possible errors, it should be remarked that our model approach presumes a liquid surface which is just flat. This ideal topography seems not to exist in our solutions. Angle-dependent measurements showed that on a microscopic scale the surface of the liquid is rough [15, 16]. Furthermore, the measurements gave evidence that a certain amount of the counter ions in the outermost layer at a certain depth is uncovered with solvent molecules and is directly accessible to the He projectiles. Principally, our model approach also enables the consideration of a more complex surface structure. However, this attempt is beyond the scope of this paper.

4.2. Variable dielectric permittivity in the surface layer

In a further attempt we tried to go beyond the simple model of constant dielectric permittivity inside the surface layer. We took into consideration that the dielectric permittivity is generally influenced by two quantities: the concentration of the salt ions and the macroscopic electric field strength in the layer. Both electrostatic interactions between solvent molecules and ions in the surface layer and the electric field strength resulting from the spatial separation of cations and anions inside this layer constrain the free rotation of solvent molecules. This constraint reduces the dielectric permittivity. Furthermore, the segregation of ions displaces polar solvent molecules, leading to an additional loss in the dielectric permittivity. To get an impression of the concentration influence we plotted the dielectric permittivity ε_S found (see table 1) against the sum of the maximum concentrations of both salt ions in the surface layer (see figure 7).

Figure 7 shows that the dielectric permittivity decreases with increasing concentration. The decrease can be described by a single exponential function in a good approximation, as depicted in the figure. On the other hand, the influence of the macroscopic field strength in the surface layer on the dielectric permittivity appears to be negligible. A calculation shows that the electric field strength in the immediate vicinity of an ion is significantly larger than the maximum field strength found in the surface layer of about 10^8 V m^{-1}. Thus, the mobility of the solvent molecules and the dielectric permittivity are more influenced by the presence of ions than by the overall electric field strength in the surface layer. Further evidence for a minor influence of the macroscopic field strength is that, although the maximum field strengths in the surface layer of the single TBPX salt solutions vary only slightly, the calculated mean dielectric permittivities of the salts are distinctly different from each other.

The concentration influence on the dielectric permittivity can be understood by assuming that any ion binds polar solvent molecules in its solvation shell and, thus, reduces their ability to orient under the influence of an external electric field. A further decrease in the orientation part of the dielectric permittivity results from the displacement of solvent molecules by the salt ions in the surface layer. The permittivity ε can be regarded as sum of two effects, orientation and electronic polarization: $\varepsilon = \varepsilon^{\text{orient}} + \varepsilon^{\text{el}}$. The latter term is hardly affected by dissolved ions while the orientation polarization is influenced by the ions.

The results shown in figure 7 suggest an exponential dependence of the dielectric permittivity on the ion concentrations. Therefore, we introduce the following model equation,

$$\varepsilon(c_1, c_2) = \varepsilon^{\text{orient}}(0, 0) \exp(-k_1 c_1 - k_2 c_2) + \varepsilon^{\text{el}}, \tag{5}$$

assuming that two ions with the concentrations c_1 and c_2 govern the dielectric permittivity and that the addition of orientation and electronic polarization of matter is a good approximation.

According to equation (5), the orientation part of the permittivity drops exponentially from the permittivity value of the pure solvent $\varepsilon^{\text{orient}}(0, 0)$ to the electronic part ε^{el}.

The following model assumption is suited to justify the above exponential dependence on ion concentrations. We assume that the two ions have the ability to block the reorientation of solvent molecules. This immobilization and the above-mentioned displacement of solvent molecules by the ions can be described by a characteristic volume k_1 and k_2, respectively. If we denote the concentration of free rotating solvent molecules by $n_{\text{solv,free}}$ then we can express the change of this quantity due to the variation of the ion concentration c_1 and c_2 as

$$\mathrm{d}n_{\text{solv,free}} = -n_{\text{solv,free}}(k_1 dc_1 + k_2 dc_2). \tag{6}$$

Here the concentration of free rotating solvent molecules is to be considered as a function of the two ion concentrations $n_{\text{solv,free}}(c_1, c_2)$. The separation of both variables and the subsequent integration of the resulting differential equation from zero ion concentration (0, 0) to (c_1, c_2) yields

$$n_{\text{solv,free}}(c_1, c_2) = n_{\text{solv,free}}(0, 0) \exp(-k_1 c_1 - k_2 c_2). \tag{7}$$

If we consider the orientation part of the permittivity to be proportional to the concentration of free rotating solvent molecules

$$\varepsilon^{\text{orient}}(c_1, c_2) \propto n_{\text{solv,free}}(c_1, c_2) \tag{8}$$

then we get

$$\varepsilon^{\text{orient}}(c_1, c_2) = \varepsilon^{\text{orient}}(0, 0) \exp(-k_1 c_1 - k_2 c_2) \tag{9}$$

or equation (5) for the total dielectric permittivity which includes the electronic part of the permittivity. In the case of low ion concentrations, equation (5) simplifies to

$$\varepsilon(c_1, c_2) = \varepsilon^{\text{orient}}(0, 0)(1 - k_1 c_1 - k_2 c_2) + \varepsilon^{\text{el}}. \tag{10}$$

This relation has been observed experimentally.

We used equation (5) for the calculation of the ion influence on the dielectric permittivity in the surface layer. This influence is governed by the two k-parameters. The estimation of these parameters requires suited conditional equations which can be derived from the Poisson equation. The integration of this equation by inclusion of the permittivity into the integrand yields

$$E(z) = -\frac{1}{\varepsilon_0}\int_{-\infty}^{z}\frac{1}{\varepsilon(z')}\rho(z')\,\mathrm{d}z'. \tag{11}$$

It is obvious that this expression leads to $E(-\infty) = 0$. However, the electric field strength must vanish outside the electric double layer on both sides. Thus, we have to ensure that

$$E(\infty) = -\frac{1}{\varepsilon_0}\int_{-\infty}^{\infty}\frac{1}{\varepsilon(z)}\rho(z)\,\mathrm{d}z = 0. \tag{12}$$

In case of the relative permittivity being constant this condition is identical to requirement of charge neutrality.

$$0 = \int_{-\infty}^{\infty}\rho(z)\,\mathrm{d}z. \tag{13}$$

However, if the permittivity must be considered to vary through the double layer—as is the case here—equation (13) must be satisfied independently. We define

$$R(z) = \int_{-\infty}^{z}\rho(z')\,\mathrm{d}z' \tag{14}$$

which leads to $R(-\infty) = 0$ and $R(\infty) = 0$. Via partial integration of equation (12) we obtain

$$0 = \frac{1}{\varepsilon_0}\int_{-\infty}^{\infty}\rho(z)\frac{1}{\varepsilon(z)}\,\mathrm{d}z = \frac{1}{\varepsilon_0}R(z)\frac{1}{\varepsilon(z)}\bigg|_{-\infty}^{\infty} - \frac{1}{\varepsilon_0}\int_{-\infty}^{\infty}R(z)\frac{\mathrm{d}}{\mathrm{d}z}\left(\frac{1}{\varepsilon(z)}\right)\mathrm{d}z. \tag{15}$$

Equation (15) can be further simplified. Thus, equation (12) is equivalent to the following equation:

$$0 = \int_{-\infty}^{\infty}R(z)\frac{\mathrm{d}}{\mathrm{d}z}\left(\frac{1}{\varepsilon(z)}\right)\mathrm{d}z, \tag{16}$$

which represents a side condition for the spatial dependence of the relative permittivity.

Now we investigate the situation further for a salt consisting of a cation and an anion with the following parameterization:

$$\varepsilon(z) = \varepsilon_{\mathrm{orient}}\exp(-k_{\mathrm{cat}}c_{\mathrm{cat}} - k_{\mathrm{an}}c_{\mathrm{an}}) + \varepsilon_{\mathrm{el}}. \tag{17}$$

The derivative of the reciprocal permittivity is then evaluated as

$$\frac{\mathrm{d}}{\mathrm{d}z}\left(\frac{1}{\varepsilon(z)}\right) = -\left(-k_{\mathrm{cat}}\frac{\mathrm{d}c_{\mathrm{cat}}}{\mathrm{d}z} - k_{\mathrm{an}}\frac{\mathrm{d}c_{\mathrm{an}}}{\mathrm{d}z}\right)\frac{\varepsilon_{\mathrm{orient}}\exp\left(-k_{\mathrm{cat}}c_{\mathrm{cat}} - k_{\mathrm{an}}c_{\mathrm{an}}\right)}{\left(\varepsilon_{\mathrm{orient}}\exp\left(-k_{\mathrm{cat}}c_{\mathrm{cat}} - k_{\mathrm{an}}c_{\mathrm{an}}\right) + \varepsilon_{\mathrm{el}}\right)^2}. \tag{18}$$

Inserting this expression into equation (16) yields

$$0 = \int_{-\infty}^{\infty}R(z)\left(k_{\mathrm{cat}}\frac{\mathrm{d}c_{\mathrm{cat}}}{\mathrm{d}z} + k_{\mathrm{an}}\frac{\mathrm{d}c_{\mathrm{an}}}{\mathrm{d}z}\right)\frac{\varepsilon_{\mathrm{orient}}\exp\left(-k_{\mathrm{cat}}c_{\mathrm{cat}} - k_{\mathrm{an}}c_{\mathrm{an}}\right)}{\left(\varepsilon_{\mathrm{orient}}\exp\left(-k_{\mathrm{cat}}c_{\mathrm{cat}} - k_{\mathrm{an}}c_{\mathrm{an}}\right) + \varepsilon_{\mathrm{el}}\right)^2}\mathrm{d}z. \tag{19}$$

The static permittivity has positive values under all conditions. Thus, the factor

$$\frac{\varepsilon_{\mathrm{orient}}\exp\left(-k_{\mathrm{cat}}c_{\mathrm{cat}} - k_{\mathrm{an}}c_{\mathrm{an}}\right)}{\left(\varepsilon_{\mathrm{orient}}\exp\left(-k_{\mathrm{cat}}c_{\mathrm{cat}} - k_{\mathrm{an}}c_{\mathrm{an}}\right) + \varepsilon_{\mathrm{el}}\right)^2}$$

is positive in the full interval of integration. Accordingly, it is possible to find a positive constant by which this factor can be replaced in the integrand without changing the value of the integral. This leads in a straightforward way to the condition

$$0 = \int_{-\infty}^{\infty}R(z)\left(k_{\mathrm{cat}}\frac{\mathrm{d}c_{\mathrm{cat}}}{\mathrm{d}z} + k_{\mathrm{an}}\frac{\mathrm{d}c_{\mathrm{an}}}{\mathrm{d}z}\right)\mathrm{d}z. \tag{20}$$

Table 2. Analysis of the k-parameters which govern the ion influence on the dielectric permittivity. The k-parameter given for TPB^+ is the mean value of all TPB^+ k-parameters shown in figure 9 (see the text for details).

Ion	r_{ion} (Å)	k (l mol^{-1})	V_t (Å^3/ion)	N
TBP^+	4.78	1.38	2300	28
I^-	2.16	0.5	830	12
Br^-	1.96	1.26	2090	31
Cl^-	1.81	1.03	1710	25

Equation (20) can be used as a conditional equation for determining the k-parameters. A second equation results from the comparison of the measured surface potential φ with the surface potential calculated by using Poisson's equation. The integration of equation (3) by inclusion of the dielectric permittivity into the integrand yields

$$\varphi = -\frac{1}{\varepsilon_0}\int_{-\infty}^{+\infty}\left(\int_{-\infty}^{z}\frac{\rho(z')}{\varepsilon_{orient}\exp(-k_{cat}c_{cat}-k_{an}c_{an})+\varepsilon_{el}}\,dz'\right)dz''. \tag{21}$$

Equations (20) and (21) are sufficient to determine k_{cat} and k_{an} by numerical integration.

Figures 8(a)–(c) show the depth profiles of the field strength and the surface potential calculated with variable dielectric permittivities in the surface layer.

Figure 9 shows the k-parameters obtained for the ions under study.

It is obvious that the cationic parameters k_{cat} of the three salts differ only slightly, while the anionic parameters k_{an} appear to vary over a large range. These results agree with the expectations. All investigated salts contain the same cation (TBP^+) but different anions which should have different k-parameters. The error bars shown in figure 9 are calculated by consideration of the errors of both the measured surface potential (± 10 mV) and the depth position of the ion depth profiles (± 0.7 Å), respectively. To estimate the position error we displaced the cationic depth profile either slightly towards vacuum or to the bulk of the solution and noticed the deviation in the k-parameters from the k-parameter without any shift of an ion depth profile.

The k-parameters obtained can be used to estimate the number of solvent molecules in the surrounding of an ion. These solvent molecules are electrostatically influenced by the salt ions and contribute to the loss of the dielectric permittivity in the surface layer.

As mentioned above, the k-parameters represent the characteristic volumes of the ions in l mol^{-1}. The characteristic volumes can be recalculated into the total volume V_t occupied by the ion itself and solvent molecules in the neighbourhood of the ion. The volumes of these solvent molecules are obtained by subtraction of the ion volume from the total volume. Hence, the number of solvent molecules N in the surrounding of an ion can be estimated by using the volume of the formamide molecule (66.1 Å^3). Table 2 gives the results of the calculations.

Table 2 shows that iodine is that anion which interacts with the least number of solvent molecules in the surface layer. The numbers of solvent molecules around bromine and iodine are considerably larger than those of iodine and differ only slightly compared to the number of solvent molecules around iodine.

4.3. Surface excess

Another quantity which can be calculated from the measured ion depth profiles is the surface excess. For the calculation we applied the concept of the Gibbs dividing plane, which is explained for example in [17]. An application of the concept to our liquid interfaces is given

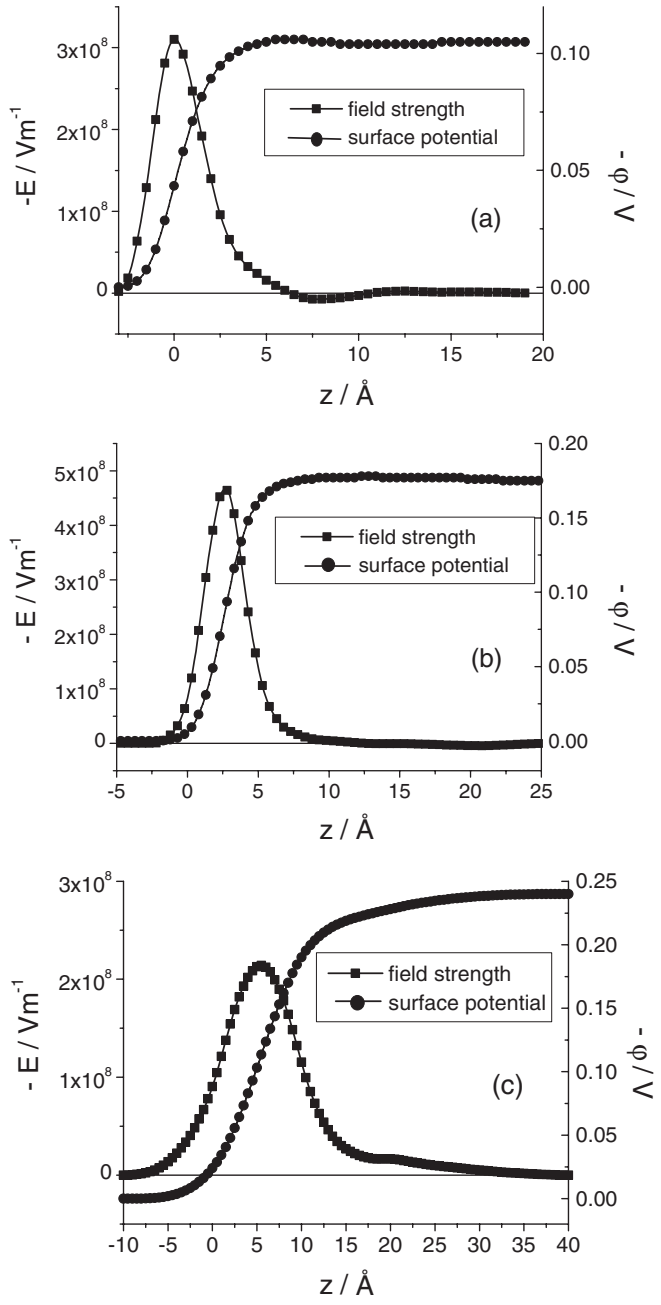

Figure 8. Depth course of the calculated field strength and the electrical potential in the surface layer of formamide solutions of 0.25 molal tetrabutylphosphonium iodide (curve (a)), 0.25 molal tetrabutylphosphonium (curve (b)) and 0.25 molal tetrabutyl-phosphonium chloride (curve (c)).

in [18]. The finding of the position z_0 of the Gibbs dividing plane requires information about the depth profile of the solvent. This information can be extracted from the oxygen step in the time of flight spectra (see figure 3). The element oxygen which is only present in the liquid

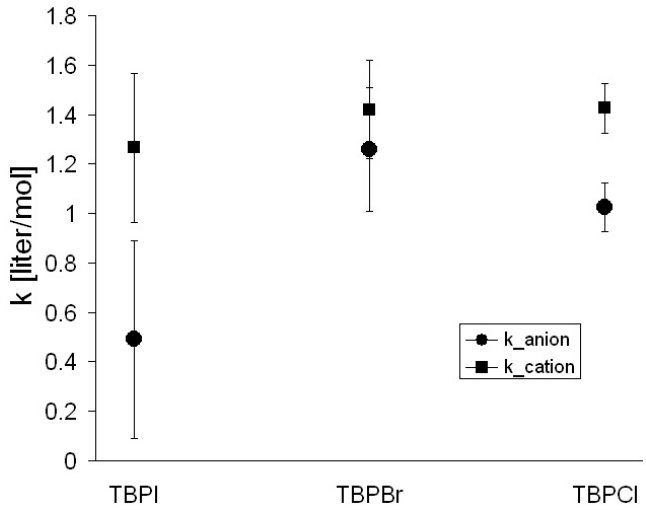

Figure 9. Calculated k-parameters for the ions of the tetrabutylphosphonium salts. The k-parameters govern the ion influence on the dielectric permittivity of salt solutions.

indicates our solvent formamide. The surface excess Γ_i is calculated according to the following equation:

$$\Gamma_i = \int_{-\infty}^{z_0} c_i(z)\,\mathrm{d}z + \int_{z_0}^{\infty} (c_i(z) - c_i^{\mathrm{b}})\,\mathrm{d}z \tag{22}$$

with the ion concentration $c(z)$ at depth z and the bulk ion concentration c_i^{b}. The position z_0 of the Gibbs dividing plane was estimated as 2 Å for the salt solutions used. The integration of the ion depth profiles in figure 5 according to equation (22) yields the surface excess listed in table 1.

The table shows that the magnitude of surface concentration excess depends on the tetrabutyl-onium salt used and especially on the anion of the salt.

5. Summary and discussion

The NICISS measurements on solutions of surface-active TBPX salts reveal a picture of the interfacial double layer which differs from that generally assumed for liquids containing ionic surfactants. There is no layer formed exclusively of surface-active ions which govern the ion distribution in the adjacent layer. We found that the depth profiles of the surface-active cation and of the counter anion are overlapped in a large depth range. For all salts under study, the profiles of the surface-active cation was found to be closer to the surface than the depth profiles of the anion. The measurements reveal that the difference between the centres of gravity of both salt ions depends on the anion of the surface-active salt. The largest difference is observed for TBPCl.

The arrangement of the ions in the surface layer causes an electric surface potential which has been measured. The measured potential is used to get information about the dielectric permittivity near the surface. In a first approach we have calculated the mean dielectric permittivity in the surface layer of the different TBPX salt solutions and found that the permittivity increases in the sequence TBPI < TBPBr < TBPCl. Thus, the interface of the TBPCl solution is the most polar one of all investigated solutions. This result can be explained

with the relative large number of polar solvent molecules in the surface layer of the TBPCl solution due to the low surface excess of the salt ions and the relatively large thickness of the surface layer in this case.

In a further approach we have considered the dielectric permittivity to depend on the ion concentrations in the surface layer. In order to describe the concentration dependence of the dielectric permittivity we have introduced an exponential model approach. The approach contains two parameters which govern the individual influences of the cation and the anion on the dielectric permittivity. The parameters were estimated for the different salts used in this study. With the help of these parameters the drop of the dielectric permittivity from the large value in the bulk of the salt solution towards the low value adjacent to the surface can be calculated.

Furthermore, the analysis of these parameters provides the specific volume which is influenced by a salt ion in the surface layer. This volume yields the number of solvent molecules N in the neighbourhood of an ion. These molecules contribute to the loss of permittivity in the surface layer due to the restriction of their free rotation caused by electrostatic interactions with the ions. We found that the number of solvent molecules N around the iodide is considerably smaller than those of the bromide and chloride. This means that the iodide obviously undergoes a considerable loss of solvent molecules during its accommodation into the surface layer in contrast to the bromide and chloride. This fits the observation that iodide is the anion which approaches the surface best. This approach is apparently connected with a loss of solvent molecules in the neighbourhood of iodide.

The drop of the permittivity in the surface layer enhances the generation of ion pairs. The existence of ions pairs at the surface of a solution of tetrabutylammonium iodide in formamide was experimentally proved with metastable induced electron spectroscopy some years ago [19].

The formation of ion pairs is a precondition for the transfer of ions from the polar into the non-polar phase during phase transfer catalysis. A generally accepted rule states that in solutions which have a dielectric permittivity lower than 40 the formation of ion pairs is strongly enhanced [20]. Exploratory calculations show that the permittivity always falls below this value at a certain distance (some angstroms) from the solution surface. This means with respect to phase transfer catalysis that ion pairs can already be formed in that part of the polar liquid which is adjacent to the non-polar liquid.

Acknowledgments

We are indebted to Dr G Andersson who helped to tune the NICISS machine during the early stages of the experiment. We gratefully acknowledge financial support from the German Science Foundation (DFG) via grant Mo288/29-1,2.

References

[1] Paluch M 2000 *Adv. Colloid Interface Sci.* **84** 27
[2] Stern O 1924 *Z. Elektrochem.* **30** 508
[3] Grahame D C 1954 *J. Am. Chem. Soc.* **76** 4819
[4] Su T J, Lu J R, Thomas R K and Penfold J 1997 *J. Phys. Chem.* B **1001** 937
[5] Koelch P and Motschmann H 2004 *J. Phys. Chem.* B **108** 18659
[6] Petrov M, Minofar B, Vrbka L, Jungwirth P, Koelch P and Motschmann H 2006 *Langmuir* **22** 2498
[7] Moberg R, Bokman F, Bohman O and Siegbahn H O G 1991 *J. Chem. Phys.* **94** 5226
[8] Eschen F, Heyerhoff M, Morgner H and Vogt J 1995 *J. Phys.: Condens. Matter* **7** 1961
[9] Winter B, Weber R, Schmidt P M, Hertel I V, Faubel M, Vrbka L and Jungwirth P 2004 *J. Phys. Chem.* B **108** 14558

[10] Winter B, Weber R, Hertel I V, Faubel M, Vrbka L and Jungwirth P 2005 *Chem. Phys. Lett.* **410** 222
[11] Andersson G and Morgner H 1998 *Surf. Sci.* **405** 138
[12] Andersson G and Morgner H 1993 *Nucl. Instrum. Methods Phys. Res.* B **155** 357
[13] Andersson G and Morgner H 2000 *Surf. Sci.* **445** 89
[14] Andersson G, Morgner H and Schulze K D 2002 *Nucl. Instrum. Methods Phys. Res.* B **190** 222
[15] Andersson G 2005 *Phys. Chem. Chem. Phys.* **7** 2942
[16] Andersson G, Krebs Th and Morgner H 2005 *Phys. Chem. Chem. Phys.* **7** 2948
[17] Adamson A W and Gast A P 1997 *Physical Chemistry of Surfaces* 6th edn (New York: Wiley)
[18] Andersson G, Krebs Th and Morgner H 2005 *Phys. Chem. Chem. Phys.* **7** 136
[19] Morgner H, Oberbrodhage J, Richter K and Roth K 1991 *J. Phys.: Condens. Matter* **3** 5639
[20] Dehmlow E V and Dehmlow S S 1993 *Phase Transfer Catalysis* (Weinheim: VCH)